

# A Novel Performance Model for the HSDPA with Adaptive Resource Allocation

Andreas Mäder<sup>1</sup>, Dirk Staehle<sup>1</sup>, and Hans Barth<sup>2</sup>

<sup>1</sup> University of Würzburg, Department of Distributed Systems  
Am Hubland, D-97074 Würzburg

[maeder,staehle]@informatik.uni-wuerzburg.de

<sup>2</sup> T-Systems Enterprise Services GmbH  
hans.barth@t-systems.com

**Abstract.** We propose a novel performance model for the HSDPA in presence of circuit-switched dedicated channels. The model consists of two parts: An HSDPA bandwidth model which considers the SIR distribution according to the multi-path model and the number of available channelization codes, and an analytical capacity model which integrates HSDPA and dedicated channels under assumption of adaptive resource allocation for the HSDPA. Additionally, the model considers the impact of location dependent bandwidths on the spatial user distribution. The accuracy of the model is demonstrated for an example scenario.

## 1 Introduction

Mobile network operators continue to deploy the High Speed Downlink Packet Access (HSDPA) service in their existing UMTS networks. From the users perspective, the HSDPA offers high bit rates (promised are up to 14.4 Mbps) and low latency. From operators perspective, the HSDPA is hoped to play a key role for the much longed for break through of high quality mobile data services. From a technical perspective, the HSDPA brings a new paradigm to UMTS: Instead of adapting transmit power to the radio channel condition in order to ensure constant link quality, HSDPA adapts the link quality to the radio channel conditions. This enables a more efficient use of scarce resources like transmit power, code resources and also hardware resources.

The basic principle of the HSDPA is to adapt the link to the radio channel condition with help of adaptive modulation and coding (AMC). For this reason, it employs a shared channel, the HS-DSCH, which is used by all HSDPA users. By using a shared channel, radio resources are occupied only if a transmission occurs which enables a more efficient transport of bursty traffic. In each transport time interval (TTI), the scheduler located in the NodeB decides which users will be scheduled at which rate. The scheduling decision can either be on behalf of channel quality indicator (CQI) reports from the UEs to enable opportunistic scheduling schemes which use the air interface more efficiently, or simple non-opportunistic schemes like Round-Robin can be used, which distributes the resources time-fair between the users. The rate selection in the NodeB

is done with a direct relation between CQI and the transport format resource combination (TFRC), which describes the number of information bits per TTI, the modulation scheme and following from this the code rate.

In the literature, a wide range of publications on several aspects of the HSDPA exists. The capacity of the HSDPA, mostly in terms of throughput, is the focus of many works which use simulations to obtain their results. The models in early publications like [1] and [2] concentrate on aspects of scheduling, HARQ and physical layer techniques. In [3], link-layer simulations have been performed which are used to fit the signal-to-noise ratio to CQIs. All these models do not consider the impact of coexistent dedicated channels on the HSDPA. This is done in [4], which assumes a fixed number of codes reserved for the HS-DSCH in their extensive simulation. The impact of the HSDPA on network planning is the focus of [5], [6], [7] and [8]. All these works use simulations for their results. The impact of code restraints is considered in [5] and [6], while [7] and [8] concentrate on the influence of the multi-path model and scheduling. In [9], a method for the estimation of the interference for the HSDPA is proposed.

In the next section we give a short overview of the HSDPA and relevant parts of the UMTS system. In Sec. 3, we introduce the model for the DCH users, for the HSDPA bandwidth and for the stochastic capacity model. In Sec. 5, we provide some numerical results and discuss the key impact factors on the performance of the HSDPA. Finally, in Sec. 6, we give a conclusion and point out some further topics of research.

## 2 System Description

The HSDPA is part of the UMTS Rel. 5. The core of the HSDPA is a new transport channel, the HS-DSCH (high speed downlink shared channel), which is a channel which is shared between all UEs in a sector. The HS-DSCH enables two types of multiplexing: Time multiplex by scheduling the subframes to different users, and code multiplex by assigning each user a non-overlapping subset of the available codes. Figure 1 shows a schematic view of the HS-DSCH over a short time period. The time axis is divided in subframes of 2 ms. In each subframe, one of three users is assigned a number of codes with SF 16 between 0 and 15. Throughout this work we only consider time multiplex.

In contrast to DCH, where the transmit power is adapted to the propagation loss with fast power control and thus enabling a more or less constant bit rate, the HS-DSCH adapts the channel to the propagation loss with adaptive modulation and coding (AMC). This means that depending on the received SIR, the scheduler in the NodeB chooses a transport format combination (TFC) with a pre-defined target FER (frame error rate), which is often chosen as 10%. The TFC contains information about the modulation (QPSK or 16QAM), the number of used codes (from 1 to 15), and the coding rate resulting in a certain transport block size (TBS) that defines the information bits transmitted during a TTI. Which TFC to choose is determined by a number of tables in [10] which map the channel quality indicator (CQI) to TFC. The channel quality indicator

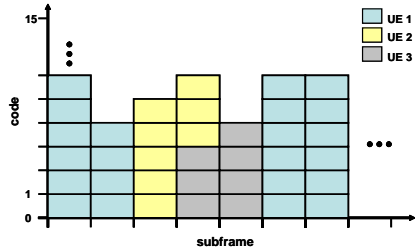


**Fig. 1.** Schematic view of the HS-DSCH

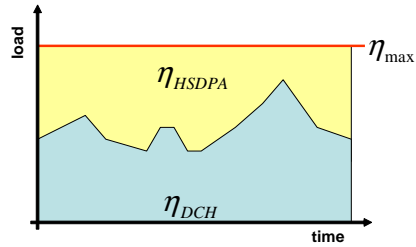


**Fig. 2.** Fast power adaptation

is a discretization of the received SIR at the UE and ranges from 0 to 30. The mapping from CQI to TFC depends on the technical capabilities of the UE and there exist five different UE classes.

Since DCH connections are power controlled and have a fixed bit rate, the load  $\eta_D$  for DCH connections depends on the other-cell interference, on the bit rates and on the number of connections only. The unused resource (i.e. transmit power) on the downlink is available for the HSDPA. We consider fast power adaptation for the HSDPA, which means that the NodeB adapts the HSDPA transmit power instantaneously on the load situation and therefore always meets a operator-defined target load  $\eta_{\max}$ , cf. Fig. 2.

### 3 System Model

#### 3.1 HSDPA Bandwidth Model

In the following we propose a simple model for computing the long-term bandwidth for a system state that provides us the number of codes and the transmit power available for the HSDPA as well as the number of users that share these resources. We assume the adaptive HSDPA configuration which means that the HSDPA uses or may use all transmit power and all codes remaining from the dedicated channels. In particular, this means that all cells are transmitting with maximum/desired power  $T_{max}$  if there is at least one HSDPA user, and in the following we make the worst-case assumption that the surrounding cells always serve an HSDPA user and consequently produce interference according to their maximum power. Furthermore, we assume the round robin scheduling discipline which gives us a direct relationship of long-term bandwidth  $R$  and mean TBS  $E[TBS]$  for a certain number  $N_{hs}$  of HSDPA users:

$$R = \frac{1s}{N_{hs} \cdot 2ms \cdot TTI} \cdot E[TBS]. \quad (1)$$

The standard specifies a set of TFCs according to the technical capabilities of the UE. A TFC relates the CQI to the TBS and the required number of parallel HSDPA codes. The CQI is a random variable that depends on the instantaneous

channel conditions. Let  $p_{CQI}(q)$  be the probability for a CQI of  $q$  corresponding to the TFC with TBS  $TBS(q)$ . For a number  $C_{hs}$  of usable HSDPA codes, we obtain the mean TBS as

$$E[TBS] = \sum_{q=0}^{30} p_{CQI}(q) \cdot \min(TBS^*, TBS(q)), \quad (2)$$

where  $TBS^*$  is the maximum TBS that is possible with  $C_{hs}$  codes. The CQI relates to the SIR in decibels according to the formula given in [3]

$$CQI = \max\left(0, \min\left(30, \left\lfloor \frac{SIR[dB]}{1.02} + 16.62 \right\rfloor\right)\right). \quad (3)$$

The SIR depends on the HSDPA transmit power  $T_{hs}$ , the location  $f$  of the mobile that defines the average propagation gain  $d_{y,f}$  from a NodeB  $y$  to the mobile, and finally the multi-path propagation. The multi-path profile for the channel between NodeB  $y$  and location  $f$  corresponds to a set of paths  $\mathcal{P}_{y,f}$ . Every single path  $p$  corresponds to a Rayleigh fading channel with an average relative power  $\beta_p$ . For numerical results we used the ITU Vehicular A model:

path $p$	1	2	3	4	5	6
average power $\beta_p$ [dB]	0	-1	-9	-10	-15	-20

Assuming optimal maximum ratio combining by the RAKE receiver, the SIR  $\gamma_f$  at a certain position  $f$  and for a certain ratio  $\Delta_T = T_{hs}/T_{max}$  of HSDPA power to total cell power is given by

$$\gamma_f(\Delta_T) = \Delta_T \cdot \sum_{p \in \mathcal{P}_{x,f}} \frac{\xi_p}{\frac{I_f^{other}}{T_{max} \cdot d_{x,f}} + \sum_{r \in \mathcal{P}_{x,f} \setminus p} \xi_r} \quad (4)$$

$$\text{with } I_f^{other} = \sum_y d_{y,f} \cdot T_{max} \cdot \sum_{r \in \mathcal{P}_{y,f}} \xi_r, \quad (5)$$

where  $\xi_p$  is an exponential random variable with mean  $\beta_p$  that describes the instantaneous propagation gain on path  $p$ . Note, that this equation neglects the thermal noise as it has almost no impact on the SIR for reasonably sized cells. Let us now introduce the variable  $\Gamma_f = \gamma_f(1)$  for the SIR with  $\Delta_T = 1$  that corresponds to the main sum in Eq. 4, and the variable  $\Sigma_f = I_f^{other}/(T_{max} \cdot d_{x,f})$  for the ratio of average other-cell received power to average own-cell received power. In the following we refer to the random variable  $\Gamma_f$  as the normalized SIR at location  $f$ . Now, we make the assumption that the distribution of the normalized SIR is a function of  $\Sigma_f$ . Simulations have shown that for  $\Sigma_f < 0.1$  the distribution of  $\Gamma_f$  in decibel scale is well-approximated by an inverse Gaussian distribution and for  $\Sigma_f \geq 0.1$  the distribution of  $\Gamma_f$  in linear scale is also well-approximated by an inverse Gaussian distribution. Based on the assumption that the distribution of  $\Gamma_f$  is a function of  $\Sigma_f$  we identified the following functions

for the mean and standard deviation of  $\Gamma_f$ :

$$\begin{aligned} E[\Gamma_f] &= 0.1424 + 4.0627 \cdot \exp(-2.0073 \cdot \Sigma_f^{0.4220}), \text{ for } \Sigma_f \geq 0.1 \\ STD[\Gamma_f] &= 0.1283 + 5.7680 \cdot \exp(-3.0712 \cdot \Sigma_f^{0.2819}), \text{ for } \Sigma_f \geq 0.1 \\ E[\Gamma_f[dB]] &= 0.0807 + 3.9085 \cdot \exp(-4.3624 \cdot \Sigma_f^{0.9728}), \text{ for } \Sigma_f < 0.1 \\ STD[\Gamma_f[dB]] &= 1.1039 + 1.2365 \cdot \exp(-0.7480 \cdot \Sigma_f^{0.4109}), \text{ for } \Sigma_f < 0.1 \end{aligned} \quad (6)$$

The probability density function (PDF)  $a(x)$  of an inverse Gaussian distributed random variable  $X$  is given by

$$a(x) = \sqrt{\frac{\lambda}{2\pi x^3}} \cdot e^{-\frac{\lambda(x-\mu)^2}{(2x\mu^2)}} \text{ with } \mu = E[X] \text{ and } \lambda = \frac{E[X]^3}{VAR[X]}. \quad (7)$$

Consequently, we are now able to determine the PDF  $a_{\Gamma_f}(x)$  of the normalized SIR at a certain location  $f$  that corresponds to the ratio of average other- and own-cell received powers. Applying the formula in Eq. (3) that relates SIR to CQI we obtain the following distribution for the CQI:

$$p_{CQI}(q, f) = \begin{cases} A_{\Gamma_f}(\phi_{max}(q)), & \text{for } q = 0 \\ A_{\Gamma_f}(\phi_{max}(q)) - A_{\Gamma_f}(\phi_{min}(q)), & \text{for } q = 1, \dots, 29 \\ 1 - A_{\Gamma_f}(\phi_{min}(q)), & \text{for } q = 30 \end{cases} \quad (8)$$

where  $A_{\Gamma_f}$  denotes the CDF of the normalized SIR and the functions  $\phi_{max}(q)$  and  $\phi_{min}(q)$  relate to the maximum and minimum normalized SIR for a certain HSDPA power that lead to CQI  $q$ . The functions are given as

$$\begin{aligned} \phi_{max}(q) &= (q - 15.62) \cdot 1.02 + \Delta_T[dB] \\ \phi_{min}(q) &= (q - 16.62) \cdot 1.02 + \Delta_T[dB]. \end{aligned} \quad (9)$$

Now, Eq. (8) yields the distribution of the CQI to be used in Eq. (2) and Eq. (1) for computing the mean TBS and the long-term bandwidth  $R_f(C_{hs}, \Delta_T)$  of an HSDPA user at a certain position  $f$  within the cell area, a ratio  $\Delta_T$  of HSDPA power to total cell power, and  $C_{hs}$  available HSDPA codes.

In the following, we demonstrate the accuracy of the model. Therefore, we consider a network with 19 hexagonal cells arranged in two tiers around a central cell. The distance between two NodeBs is 1.2 km. For this network we produce 1000 random situations that means a random mobile position within the central cell and independent total transmit powers for the 19 NodeBs which are uniformly distributed between 2 W and 10 W. For every situation we generate 10000 independent instances of the multi-path profile and compute the resulting normalized SIR according to Eq. (4). Thus, we obtain the mean, the standard deviation, and the distribution of the normalized SIR, and also the associated ratio of average other- to own-cell received power for every situation. Figure 3 demonstrates the accuracy of the functions for estimating the mean and the standard deviation of the normalized SIR as defined in Eq. (6). The left figure shows the functions for  $\Sigma < 0.1$  and the right figure for  $\Sigma \geq 0.1$ . The functions displayed as solid lines match the center of the simulated points which mark the 1000 different situations quite well. The deviation of the simulated points

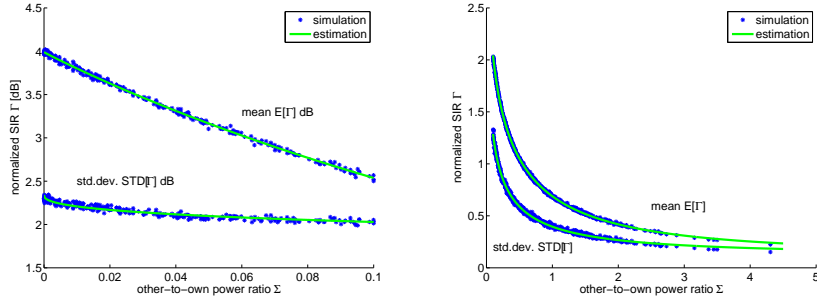


**Fig. 3.** Accuracy of the functions defined in Eq. (6).

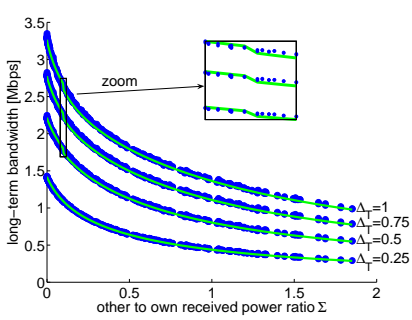


**Fig. 4.** Accuracy of long-term bandwidth estimation.

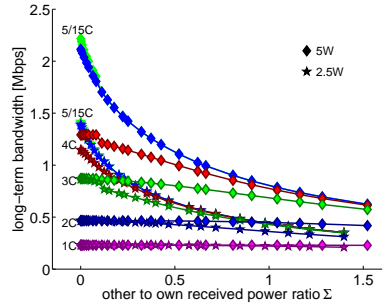


**Fig. 5.** Impact of codes and power on long-term bandwidth. (xC means x HSDPA codex)

from the estimated function results from the fact that the distribution of the normalized SIR is precisely a function of all received powers and the aggregation of these values to the single value  $\Sigma$  is an approximation leading to a certain inaccuracy.

Next, we demonstrate the final accuracy of the long-term bandwidth estimation for a more specific scenario. The values of  $\Sigma$  correspond to points on a grid with a resolution of 50m covering the central cell. Furthermore, we apply now the adaptive HSDPA configuration, which means that all cells transmit with equal power. The ratio  $\Delta_T$  of HSDPA power to total cell power is set to 1/4, 1/2, 3/4, and 1. The maximum of 15 parallel HSDPA codes is available. Figure 4 compares the estimated bandwidth displayed as solid lines with the bandwidth resulting from the simulations presented by dot markers. We can observe a very good match for all points. The main inaccuracy occurs for values of  $\Sigma$  around 0.1 which is specifically illustrated in the small box. For  $\Sigma$  just below 0.1 we underestimate the bandwidth and for values just above 0.1 we overestimate the bandwidth. The switching point is exactly where we change estimating the dis-

tribution of  $\Gamma$  from linear scale to decibel scale. Figure 5 shows the impact of available power and available codes on the HSDPA bandwidth for a single user. The power is set to 2.5 W and 5 W, the available codes are varied from only a single code up to 15 codes. The first point to observe is that in the considered scenario, i.e. full other-cell power, multi-path profile, and UE class four, five parallel codes are enough to achieve the maximum bandwidth if the HSDPA transmits with 5 W which is half of the total cell power assumed here with 10 W. On the other hand, if we have only one or two codes available, there is only a small difference in the resulting bandwidth whether the HSDPA uses 2.5 W or 5 W. For three and four codes there is a distinct gap between HSDPA powers of 2.5 W and 5 W, and up to a maximum of five, the availability of more codes also leads to an improved performance.

### 3.2 Sharing Resources between DCH and HSDPA

The main difference between a DCH and an HSDPA users is that the former receives a certain QoS expressed as the data rate  $R_s$  and the target bit-energy-to-noise ratio ( $E_b/N_0$ )  $\varepsilon_s$  while the latter utilizes the remaining resources. The data rate and the  $E_b/N_0$  value correspond to a certain spreading factor  $SF_s$  and a certain transmit power that depends on the location of the user. Applying the adaptive HSDPA configuration, i.e. the HSDPA consumes all power remaining from the DCH users and accordingly all NodeBs transmit with target power  $T_{\max}$ , the power requirement for DCH users is given by the following equation, which follows from the  $E_b/N_0$ -equation for power controlled CDMA systems:

$$\hat{T}_k = \frac{\varepsilon_s R_s}{W} \cdot \left( W N_0 \cdot \frac{1}{d_{x,k}} + \sum_{y \neq x} T_{\max} \cdot \frac{d_{y,k}}{d_{x,k}} + \alpha \cdot T_{\max} \right), \quad (10)$$

where  $\alpha$  is the orthogonality factor,  $W$  is the system chip rate, and  $N_0$  is the thermal noise density. Neglecting thermal noise, we define the mean load of one DCH user as its transmit power divided by the maximum cell power:

$$\omega_s = \nu_s \cdot \frac{\varepsilon_s R_s}{W} \cdot \left( \sum_{y \neq x} E \left[ \frac{d_{y,k}}{d_{x,k}} \right] + \alpha \right), \quad (11)$$

where  $\nu_s$  is the activity factor. The total DCH load  $\eta_d$  and the mean HSDPA transmit power are then given by

$$\eta_D = \sum_{s \in \mathcal{S}} n_s \omega_s, \quad \text{and} \quad T_H = T_{\max} - T_c - \eta_D \cdot T_{\max}, \quad (12)$$

where  $T_c$  is the power required for common channels.

The UMTS downlink uses orthogonal variable spreading factor (OSVF) codes with spreading factors (SF) between 4 and 512. If we use the code  $c_{512}$  with SF 512 as the basic code unit, all other codes can be expressed in terms of a multiple of  $c_{512}$ , such that  $c_s = \frac{512}{SF_s}$ . With the assumption of perfect re-ordering the system has a total code capacity  $C$  of  $512 - c_c$ , where  $c_c = 32$  is reserved for common channels. The HSDPA is able to use multiple codes with spreading factor 16 in parallel. Accordingly,  $C_{hs} = \left\lfloor \frac{480 - \sum_s n_s \cdot c_s}{32} \right\rfloor$  HSDPA codes are available.

## 4 Capacity Model

We consider a UMTS cell with users arriving according to a Poisson process with rate  $\lambda_s$  for DCH users and  $\lambda_H$  for HSDPA users. DCH users depart with rate  $\mu_s$  and have exponentially distributed service times whereas HSDPA users transmit an exponentially distributed data volume with mean  $E[V_H]$ . The user location is uniformly distributed over the cell area which is divided into a number  $q$  of square area units. We develop a common state space for DCH and HSDPA traffic in order to estimate the performance of the HSDPA.

We consider the number of occupied code units as state space description. Each DCH service connection requires a number  $c_s$  of SF 512 code equivalents, so the code resources form a shared resource which can be used in the Kaufman-Roberts recursion [11] to form an one-dimensional state space. However, since we also want to include the HSDPA users in the state space, we construct an 2-dimensional state space with the number of occupied code resources by DCH users on the first dimension, and the number of active HSDPA flows on the second dimension. A state  $j$  in the DCH dimension corresponds to the number of occupied code units  $c_u = \min_s(c_s)$ , i.e. in state  $j$  the DCH users occupy  $j \cdot c_u$  codes with SF 512. The size of the state space is  $C/c_u \times n_{H,max}$ , where  $n_{H,max}$  is the maximum number of HSDPA users. Note that we assume here a simple count-based admission control for the HSDPA. Figure 6 shows a fraction of the state space. The departure rates for the DCH dimension are calculated according to the following equation (see [11]):

$$\tilde{\mu}_s(j) = \mu_s \cdot E[n_s|j], \quad (13)$$

where  $E[n_s|j]$  is the mean number of service class  $s$  connections in state  $j$ :

$$E[n_s|j] = \frac{\lambda_s}{\mu_s} \cdot \frac{\tilde{p}_{kr}(j - \frac{c_s}{g_c})}{\tilde{p}_{kr}j}. \quad (14)$$

The variable  $\tilde{p}_{kr}(j)$  denotes the un-normalized probability for the DCH state  $j = \frac{C}{g_c}$ . It is calculated recursively as

$$\tilde{p}_{kr}(j) = \frac{g_c}{C} \sum_{s \in S} \frac{\lambda_s}{\mu_s} c_s \tilde{p}_{kr}(j - \frac{c_s}{g_c}). \quad (15)$$

Note that this model does not allow an explicit computation of the DCH load in a state but only its mean value. This prohibits the computation of soft blocking probabilities, i.e. blocking due to transmit power limitation, for DCH users. However, in [12] it has been shown that the code capacity is the dominating factor for the system capacity except for nearly full DCH activity and concurrent bad orthogonality conditions, i.e. high orthogonality factors. Nevertheless, incorporating soft blocking and investigating the impact of the DCH load distribution within a code-based system state will be an item for future work.

The HSDPA user throughput depends on both the current DCH load and on the number of active HSDPA flows. While the code resources are directly

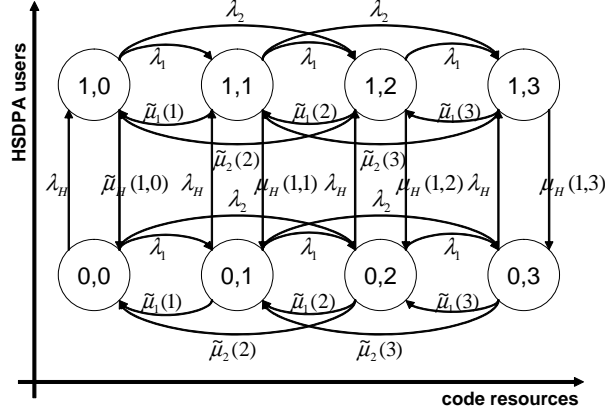


Fig. 6. Structure of a two-dimensional state space

available through the state, the current transmit power for the HSDPA requires knowledge of the DCH downlink load, which is calculated as in (12) using the mean number of DCH users  $E[n_s|j]$ . Consequently, the number of usable HSDPA codes is  $C_{hs}(j, n_H) = \lfloor (480 - j * c_u) / 32 \rfloor$  and the mean ratio of HSDPA power to total cell power is

$$\Delta_T(j, n_H) = 1 - \frac{T_c}{T_{\max}} - \sum_s E[n_s|j] \cdot \omega_s. \quad (16)$$

The HSDPA bandwidth for a certain location  $f$  follows according to the model defined in Section 3.1

$$R_f(j, n_H) = R_f(C_{hs}(j, n_h), \Delta_T(j, n_H)). \quad (17)$$

A straightforward method for computing the departure rate would be to determine the mean bandwidth for an HSDPA user by averaging over the cell area. We will later refer to this approach as the “naïve” approach. However, we have to consider the following: With a volume-based user model, the life-time of an HSDPA user depends on its data volume  $V_H$  and its bandwidth. Even with round-robin scheduling, users at the cell border receive a smaller bandwidth than users in the cell center, and accordingly, they stay in the system for a longer time. Consequently, the probability  $p_f$  to meet a user at position  $f$  when looking into the system at a random instance of time is larger for a location  $f$  close to the cell border than for one close to the cell center. More precisely, the probability  $p_f$  is proportional to the reciprocal bandwidth available at this position:  $p_f \sim \frac{1}{R_f(j, n_H)}$ . This effect is also mentioned by Litjens et al [8] regarding Monte Carlo simulations. We approximate the mean time  $E[T|j]$  by summing over all positions in the cell and, after some algebraic operations, obtain the

following formulation:

$$E[T|j] = E[V_H] \cdot E \left[ \frac{1}{R_f(j, n_H)^2} \right] \cdot E \left[ \frac{1}{R_f(j, n_H)} \right]^{-1} \quad (18)$$

In the following, we will refer to this method as the “location-aware” approach. In order to calculate the steady-state distribution, we arrange the transition rate matrix  $Q$  with help of an index function  $\phi(j, n_H) \rightarrow \mathbb{N}$  according to the following rules for all valid states:

$$\begin{aligned} Q(\phi(j, n_H), \phi(j + \frac{c_s}{g_c}, n_H)) &= \lambda_s \\ Q(\phi(j, n_H), \phi(j - \frac{c_s}{g_c}, n_H)) &= \tilde{\mu}_s(j) \\ Q(\phi(j, n_H), \phi(j, n_H + 1)) &= \lambda_H \\ Q(\phi(j, n_H), \phi(j, n_H - 1)) &= \frac{1}{E[T|j]} \end{aligned} \quad (19)$$

In all other cases  $Q(i, j)$  is set to zero and  $Q(i, i)$  is set to the negative row-sum of all entries to keep the state equations balanced. The steady-state distribution is then obtained by solving  $Q \cdot \bar{\pi} = 0$  s.t.  $\sum \pi = 1$  for the state vector  $\bar{\pi}$ . Performance measures like blocking probabilities or moments of the user throughput are then calculated with help of the steady-state distribution. For example, the mean HSDPA user throughput at a random time instance is

$$E[R_U] = \sum_{(j, n_H) | n_H > 0} R_U(j, n_H) \cdot \frac{n_H \cdot \pi(\phi(j, n_H))}{\sum_{(j', n'_H) | n'_H > 0} n'_H \cdot \pi(\phi(j', n'_H))}. \quad (20)$$

## 5 Numerical Example

Let us now define an example scenario with the following parameters: We consider two DCH service classes with 128 kbps and 384 kbps. The service mix is 0.6 to 0.4. The activity factor is 0.55 for both service classes. HSDPA flows arrive with rate  $\lambda_H = 1$ . The orthogonality factor  $\alpha$  for the DCH part of the air interface model is set to 0.35 corresponding to the HSDPA bandwidth model. The distance between the NodeBs is 1.2 km and the COST 231 Hata Model is used as propagation loss model. We validate our analytical results with an event-based simulation. The simulation places new users on random locations and calculates the exact air interface load for DCH users as well as the mean bandwidth for the HSDPA users according to the method specified in Section 3.1. The users keep their positions during their life time.

Figure 7 shows the mean user throughput versus the offered DCH code load which is defined as  $a_c = \sum_{s \in \mathcal{S}} \lambda_s / \mu_s \cdot c_s / C$ . The figure shows two scenarios, one with a mean HSDPA data volume of 50 kbyte and one with 100 kbyte. The influence of the spatial user distribution can be clearly seen on the large difference between the naïve approach (square marker) and the location-aware approach (circle marker). Especially for a low DCH load the difference is nearly 50%. With location-awareness, the analytical and the simulation results match well. The curves for 50 kbyte and 100 kbyte converge with a higher offered load for

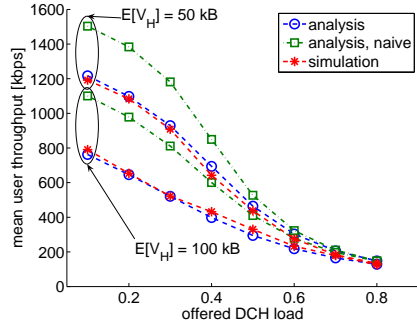


**Fig. 7.** Mean HSDPA user throughput vs. offered DCH load

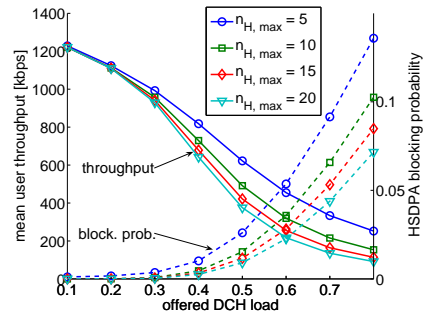


**Fig. 8.** Impact of  $n_{H,max}$  on throughput and blocking probabilities.

the DCH users since in this case the HSDPA is in an overload situation due to insufficient power and code resources.

In Fig. 8 we show the impact of the HSDPA admission control on the trade-off between user throughput and HSDPA blocking probabilities. The data volume is  $E[V_H] = 50$  kbyte. The solid lines indicate the user throughput, while the dashed lines indicate the HSDPA blocking probabilities. The maximum number of allowed HSDPA users,  $n_{H,max}$  is set to 5, 10, 15 and 20, respectively. We see that with higher DCH loads the increasing blocking probabilities for low values of  $n_{H,max}$  leads to a significant improvement of the user throughput. The difference between the curves become smaller with higher values of  $n_{H,max}$  which indicates that they will converge if  $n_{H,max}$  would be increased further.

## 6 Conclusion

We presented an analytical capacity model for the HSDPA. It includes a novel bandwidth model for the HSDPA which estimates the location dependent instantaneous user throughput with help of the SIR distribution. The model also considers DCH users, which have a crucial impact on the performance of the HSDPA both due to the transmit powers and due to the available code resources. The common state space integrates all DCH service classes into one dimension to reduce the state space dimensions and computational complexity. Furthermore, we approximated the effect of a shifted active user distribution due to location-dependent user bandwidths. The analytical results have been validated with help of a full featured simulation. The results from the simulation and the analytical results match well. Further research topics are the impact of radio resource management strategies, different multi-path profiles as well as other scheduling schemes than round robin.

## Acknowledgments

The authors want to thank Prof. Phuoc Tran-Gia, Markus Spahn and Tobias Hofffeld, University of Wuerzburg, as well as Bernhard Liesenfeld, T-Systems Germany, for the helpful discussions.

## References

1. Kolding, T.E., Frederiksen, F., Mogensen, P.E.: Performance Aspects of WCDMA Systems with High Speed Downlink Packet Access (HSDPA). In: Proc. of IEEE VTC Fall '02. Volume 1., Vancouver, Canada (2002) 477–481
2. Assaad, M., Zeglache, D.: On the Capacity of HSDPA. In: Proc. of GLOBECOM '03. Volume 1., San Francisco, USA (2003) 60–64
3. Brouwer, F., de Bruin, I., de Bruin, J., Souto, N., Cercas, F., Correia, A.: Usage of Link-Level Performance Indicators for HSDPA Network-Level Simulations in E-UMTS. In: Proc. of IEEE ISSSTA '04, Sidney, Australia (2004) 844–848
4. Pedersen, K.I., Lootsma, T.F., Støttrup, M., Frederiksen, F., Kolding, T.E., Mogensen, P.E.: Network Performance of Mixed Traffic on High Speed Downlink Packet Access and Dedicated Channels in WCDMA. In: Proc. of IEEE VTC Fall '04. Volume 6., Milan, Italy (2004) 2296–4500
5. Voigt, J., Deissner, J., Hübner, J., Hunold, D., Möbius, S.: Optimizing HSDPA Performance in the UMTS Network Planning Process. In: Proc. of IEEE VTC Spring '05. Volume 4., Stockholm, Sweden (2005) 2384–2388
6. Türke, U., Koonert, M., Schelb, R., Görg, C.: HSDPA performance analysis in UMTS radio network planning simulations. In: Proc. of IEEE VTC Spring '04. Volume 5., Milan, Italy (2004) 2555–2559
7. van den Berg, J.L., Litjens, R., Laverman, J.: HSDPA flow level performance: the impact of key system and traffic aspects. In: Proc. of MSWiM '04, Venice, Italy (2004) 283–292
8. Litjens, R., van den Berg, J.L., Fleuren, M.J.: Spatial Traffic Heterogeneity in HSDPA Networks and its Impact on Network Planning. In: Proc. of ITC 19, Beijing, China (2005) 653–666
9. Mäder, A., Staehle, D.: Interference estimation for the HSDPA service in heterogeneous UMTS networks. In: Wireless Systems and Network Architectures in Next Generation Internet, LNCS vol. 3883, Como, Italy (2005)
10. 3GPP: 3GPP TS 25.306 V6.5.0 UE Radio Access capabilities (Release 6). Technical report, 3GPP (2004)
11. Kaufman, J.: Blocking in a Shared Resource Environment. *IEEE Transactions on Communications* **29**(10) (1981) 1474–1481
12. Staehle, D.: On the Code and Soft Capacity of the UMTS FDD Downlink and the Capacity Increase by using a Secondary Scrambling Code. In: Proc. of IEEE International Symposium on Personal Indoor and Mobile Radio Communications (PIMRC), Berlin, Germany (2005)